

INFLUENCE OF GAMMA RAY AND THERMAL ANNEALING ON ZINC OXIDE AND TITANIUM OXIDE THIN FILMS CHARACTERISTICS

A. ALYAMANI^a, N. MUSTAPHA^b, T.S.ALKHURAJI^c, H. IDRIS^{d,f}

^aNational Nanotechnology Center, King Abdul-Aziz City for Science and Technology (KACST), Riyadh, Kingdom of Saudi Arabia.

^bDept. of Physics, College of Sciences, Imam Mohammad Ibn Saud Islamic University, P.O. Box 90950, Riyadh 11623, Kingdom of Saudi Arabia.

^cNational Center for irradiation, King Abdul-Aziz City for Science and Technology (KACST), Riyadh, Kingdom of Saudi Arabia.

^dDept. of Physics, College of Sciences, Imam Mohammad Ibn Saud Islamic University. Committee on Radiation and Environmental Pollution Protection, Kingdom of Saudi Arabia.

^fSudan Atomic Energy Commission, P.O. Box 3001, Sudan.

The influences of gamma ray and thermal annealing on Zinc oxide and Titanium oxide thin films characteristics have been investigated. The morphology was examined by Atomic Force Microscopy (AFM) for surface roughness and grain sizes. Optical properties such as transmission and absorption of the deposited films were investigated in the visible region, using a spectrophotometer. Energy band gap (E_g) was calculated in the visible wavelength (380-780 nm) of the as-deposited and annealed films. Irradiation of the films was performed with low gamma doses to examine their stability during their uses as protective coatings or as anodes in optoelectronic devices. It was found that the optical band gap values were slightly decreased as the radiation dose was increased. The two oxide films were annealed in air atmosphere at 350 °C for one hour and examined for the change in optical or morphological properties if any. We represent a comparative study between the physical and spectral properties of Zinc and titanium oxides prepared by a well-known physical deposition process to investigate the possibility of their uses in optoelectronic devices such as anode for organic solar cells and light emitting diodes. Even after being exposed to low gamma irradiation doses and then thermally annealed the ZnO and TiO₂ films maintained good optical, electrical and morphological properties. This made them very favorable to be used as anodes for solar cells, light emitting diodes and as protective coatings in space windows.

(Received April 3, 2019; Accepted September 24, 2019)

Keywords: Oxide thin films, Pulsed laser deposition, Optical properties, Atomic force microscopy, Thermal annealing

1. Introduction

Transparent conducting oxides (ZnO and TiO₂) thin films are conducting materials and widely utilized in opt-electrical fields such as electronic circuits, solar cells, displays and opt-electrical interfaces [1]. Newly, ZnO films have obtained considerable attention because of their possible application in various technological areas, which are referred to its wide and direct band gap and their excellent physical and chemical Characteristics [2- 6]. The elements doped ZnO

*Corresponding author: nazirmustapha@yahoo.co.uk

films have appeared novel features to be utilized in optoelectronic systems. [7]. Although there are several approaches used to deposit the ZnO films [8-9], reactive sputtering is the best method because of many advantages such as reproducibility and the possibility of getting special characteristics films. This technique is also employed to fabricate films with the desired optoelectronic and nanostructure properties. TiO₂ films were extensively investigated due to their broad applications in the optical and electrical fields. Numerous researches have been conducted to understand the relationship between experimental parameters and film characteristics and deposition process. However, magnetron sputtering technique seems to be the most appropriate because it offers more choice

in controlling deposition conditions [10]. TiO₂ and ZnO thin films have been synthesized as well by pulsed laser deposition PLD. The PLD has many benefits than other deposition processes, it allows for the control of crystalline structure, high deposition rates, and stoichiometry of the fabricated film. Furthermore, good adhesion of the deposited thin film to the substrate is obtained. In addition, the incorporation of contaminants in the growing film, which usually happens during the deposition processes, is avoided [11-12]. Hence, in this work, transparent conducting TiO₂ and ZnO thin films were deposited via pulsed laser Deposition (PLD) technique onto glass substrates in an oxygen-reactive atmosphere. The overall aim was to present a comparative study between the two oxides by investigating their morphologies; and their optical properties, study the influence of gamma irradiation and annealing in an air atmosphere at 350°C on the film properties as well as to assess the ability to use these thin films as anodes in optoelectronic devices. There are no much research details reported to assess the properties of ZnO and TiO₂ films, by using low doses of gamma irradiation, followed by thermal annealing of such films in this research field.

2. Experimental details

2.1. Substrate Cleaning Procedure

Prior to oxide thin film deposition, glass substrates were cleaned by sonication with detergent (acetone), rinsed with deionized water for 10 minutes, then dried in the oven at 110 °C for outgassing.

2.2. Thin film deposition

Immediately after drying, the ultrasonically cleaned glass substrates were transferred to the PLD system for the deposition of Zinc oxide and titanium Oxide materials (110 nm thick).

For the deposition of (ZnO) films, a Pulsed Laser Deposition source (PLD) PLD/MBE 2100 from PVD Products with KrF excimer Laser source at wavelength of 248 nm and with laser repetition rate of 10 Hz was used. Zinc oxide target was fabricated using high purity ZnO (99.98%) as received from the supplier (Sigma-Aldrich), with a target to substrate distance of 10 cm maintained during all depositions. The thin film growth chamber exhibits a base pressure of 10⁻⁶ Torr. Film growth was performed at a temperature of 300°C in an oxygen pressure of 10 mTorr for 20 minutes. Similar conditions and properties were observed in the fabrication of the TiO₂ target. The ZnO and TiO₂ films have an average thickness of 110 nm for all the samples used in our work. Thickness measurements were conducted using a Deck Tack 150.

The irradiation of TiO₂ and ZnO films were performed at King Abdul Aziz City for Science and Technology, in the Atomic Energy Institute at various irradiation doses using a ⁶⁰Co Gamma Cell GC-220 Excel (manufactured by MDS Nordion, Canada) with absorbed dose rate of 6.7 kGy/h, and at room temperature. The humidity and temperature during irradiation were kept constant with an air chiller system (turbo-Jet, Kinetics, USA) as described previously in more details [13].

Table 1 represents the deposition parameters of the ZnO and TiO₂ thin films.

Table 1. Deposition parameters maintained during the deposition of ZnO and TiO₂ thin films by pulsed laser deposition.

Growth parameter	Specification / value
Target	ZnO or TiO ₂ (99.99%)
Base pressure (torr)	10 ⁻⁶
Substrate-target (cm)	10
Oxygen pressure	10 mTorr
Wavelength (nm)	248
Laser repetition rate	10Hz
Target rotation	10 Hz
Substrate Temperature (Celsius)	300
Substrate	Glass
Thin film thickness	150 nm

2.3. Sample annealing

After deposition, the samples were divided into two sets: one for characterization as-deposited and one set to be annealed in (CARBOLITE CWF 1200 model) furnace for 1 hour at a temperature (350 °C) in air, and then characterized in order to investigate the changes in morphology or spectral properties of samples.

2.4. Atomic Force Microscopy

Atomic Force microscopy (AFM) in contact mode was used to observe the surface morphology and roughness of the films before and after annealing. Structural properties and grain sizes of the grown films were also investigated.

2.5. Spectral characterization

A spectrophotometer apparatus was used for measuring the spectral properties such as reflectance, transmission and absorption of thin films in the visible range (380 – 780 nm) for thin films deposited on glass substrates. Glass substrate was used as reference to calibrate the apparatus.

2.6. Electrical properties

The four-point probe method was used to obtain the sheet resistance R_s of the ZnO and TiO₂ films. All measurements were performed at room temperature. By assuming that the thickness of the films was uniform, the resistivity ρ of the films was calculated from the simple equation:

$$\rho = R_s d, \quad (1)$$

where d is the oxide film thickness. For each film, the average sheet resistance R_s was measured from three different positions of the film's surface.

3. Results and discussions

3.1. Optical properties

Fig. 1 shows the transmission spectra of the freshly-made TiO₂ and ZnO films deposited on glass by the PLD process. The optical spectra of TiO₂ and ZnO showed a good optical transmittance of above 75% and 90% respectively in the visible range (380-780 nm).

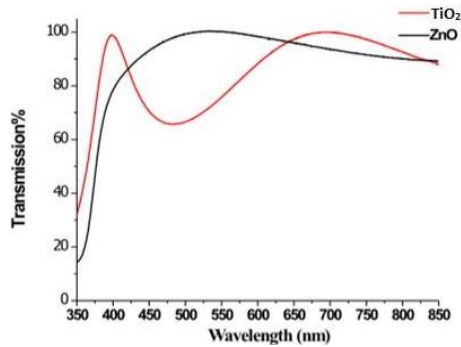


Fig. 1. The transmission spectra of the as-deposited TiO₂ and ZnO thin films.

Figs. 2 and 3 showed slight increase in the absorption spectra as a result of annealing the films at 350 °C for one hour in an air atmosphere.

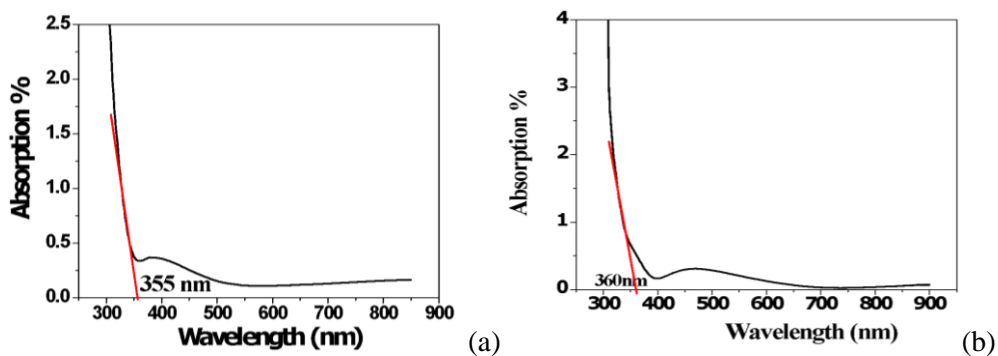


Fig. 2. The absorption spectra for the TiO₂ thin films:
(a) As-deposited and (b) annealed at 350 °C.

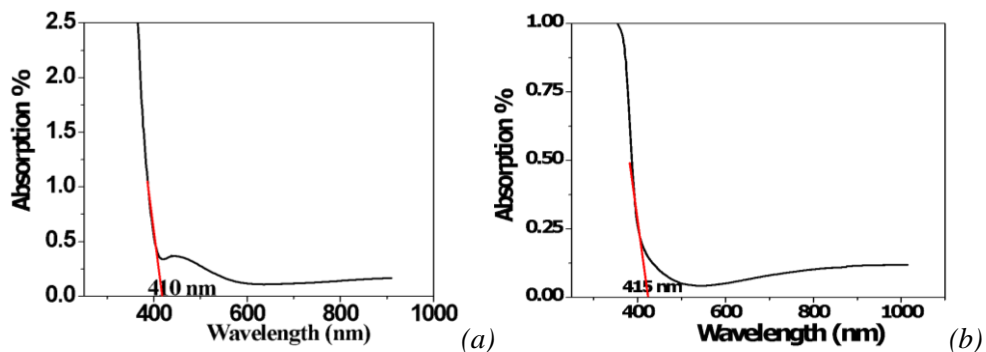


Fig. 3. Shows the absorption spectra of a ZnO film (110 nm thick):
(a) As-deposited and (b) annealed at 350 °C.

Figs. 4 and 5 showed a slight decrease of 5% for the transmittance spectra of the annealed ZnO and TiO₂ oxides. The as-deposited TiO₂ films showed a high transmission in the visible (70%) at $\lambda = 550$ nm, and in the infrared at $\lambda = 700$ nm (97%) as in Fig. 4.

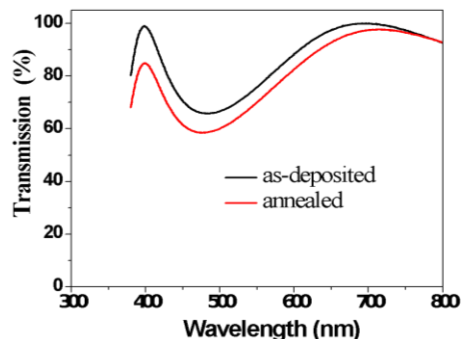


Fig. 4. Transmission spectra of the as-deposited and annealed TiO₂ thin films.

While for the ZnO, the transmission in the visible at $\lambda = 550$ nm was (96%) and around 93% in the infrared $\lambda = 700$ nm as can be seen in Fig. 5. For its application as anode in a solar cell, ZnO film must have a high transmittance in the visible range. From Fig. 5, it is clear that all ZnO films as-deposited and annealed, maintained high transmittance, up to 90%, in the visible region.

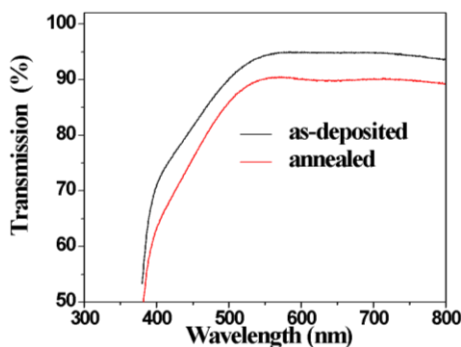


Fig. 5. Transmission spectra of the as-deposited and annealed ZnO thin films.

3.2. Atomic Force Microscopy (AFM)

Atomic Force Microscopy (AFM) was used to find the morphology and surface roughness of the as-deposited, annealed and irradiated TiO₂ and ZnO films. Fig. 6 shows the AFM surface roughness of as-deposited and annealed ZnO films respectively. As can be seen from fig.6, the roughness of the ZnO thin film, increased from 1.2 nm for the freshly made sample to 2.3 nm for annealed film at 350 °C. Fig. 7 shows the surface roughness of as-deposited and annealed TiO₂ respectively. The roughness of the TiO₂ film also increased from 0.9 nm of the freshly made sample to 1.25 nm for the annealed film at 350 °C. This can be attributed to the increase in the grain sizes of the two oxides due to the post-deposition annealing.

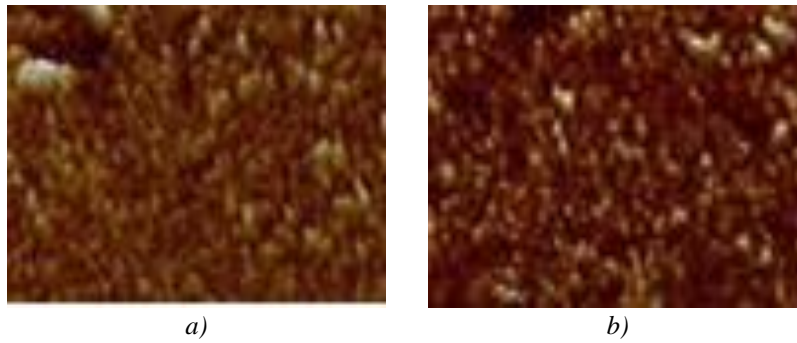


Fig. 6. AFM images of ZnO thin films.
 (a) AFM image of surface roughness for as-deposited ZnO thin film (110 nm thick).
 (b) AFM image of surface roughness for ZnO thin film (110 nm thick) annealed at 350 °C for one hour.

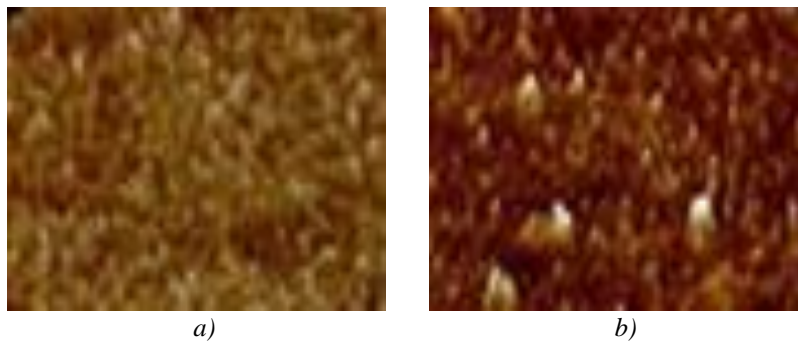


Fig. 7. AFM images of TiO₂ thin films.
 (a) AFM image of surface roughness for as-deposited TiO₂ thin film (110 nm thick).
 (b) AFM image of surface roughness for TiO₂ thin film annealed at 350 °C.

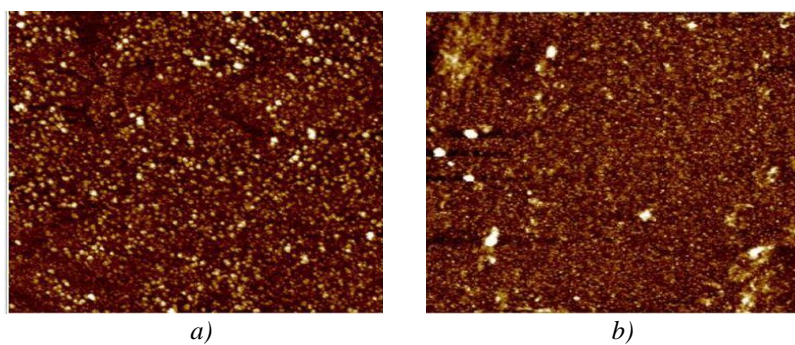
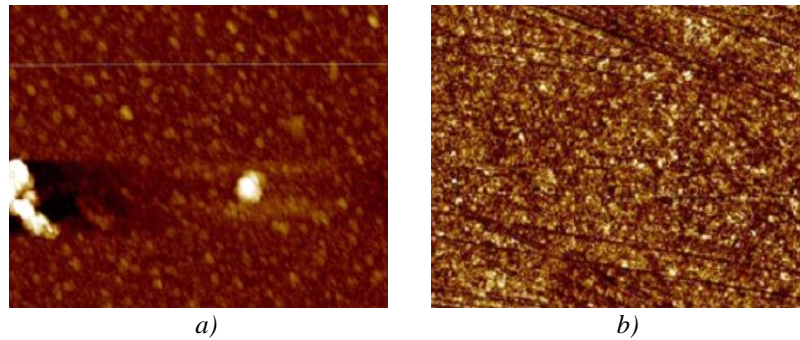


Fig. 8. AFM images of the ZnO thin films (110 nm thick).
 (a) AFM micrograph of the as-deposited ZnO thin film (for the surface morphology).
 (b) AFM micrograph of the ZnO annealed at 350 °C.



*Fig. 9. AFM images of the TiO₂ thin films.
 (a) AFM image of the as-deposited TiO₂ thin film (110 nm thick).
 (b) Morphology of the TiO₂ thin film annealed at 350 °C.*

Fig. 8 shows the AFM surface morphology images of as-deposited and annealed ZnO thin films. Fig. 8 (a) of ZnO film shows dense small grain sizes (9.5nm), while for the annealed ZnO the crystalline structure improved and the grain sizes become larger (28.5 nm) as in Fig.8(b). The morphology of the as-deposited and annealed TiO₂ films are represented in Fig. 9. Thermal annealing of TiO₂ films resulted in densification of the surface grain sizes as can be seen in fig.9.

Fig. 10 shows AFM images of the morphology of ZnO films irradiated at various gamma doses up to 25 kGy. It is clearly seen that increasing the dose rate resulted , in an increase of the grain sizes and that they agglomerated in different shapes.

Fig. 11 shows the morphology of TiO₂ films irradiated at various gamma doses (up to 25 kGy). AFM images showed the grain size of TiO₂ films decreased after gamma irradiation at low dose of 5kGy as in fig. 11.(b) and that grain size being increased after gamma irradiation of high doses 10 kGy, 20 kGy and 25 kGy as in fig. 11, (c), (d) and (e) respectively.

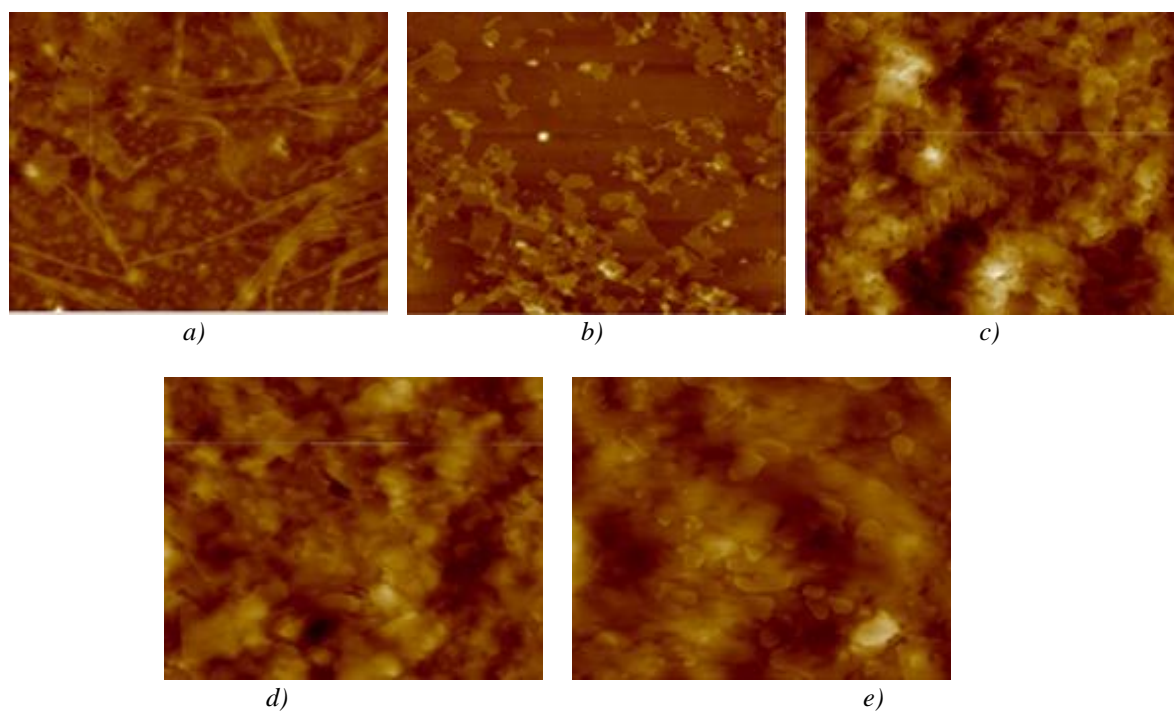


Fig. 10. The morphology of ZnO films irradiated at various gamma doses. (a) 0kGy; (b) 5kGy; (c) 10 kGy; (d) 20 kGy; (e) 25 kGy

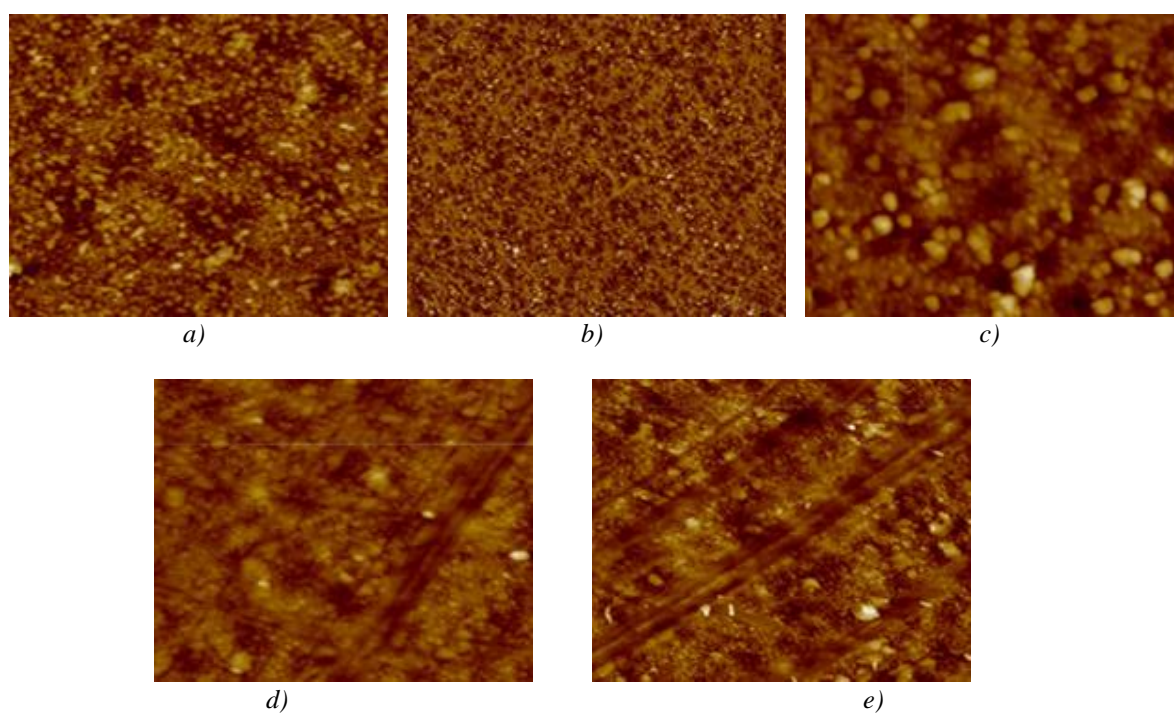


Fig. 11. The morphology of TiO₂ films irradiated at various gamma doses. (a) 0kGy; (b) 5kGy; (c) 10 kGy; (d) 20 kGy; (e) 25 kGy

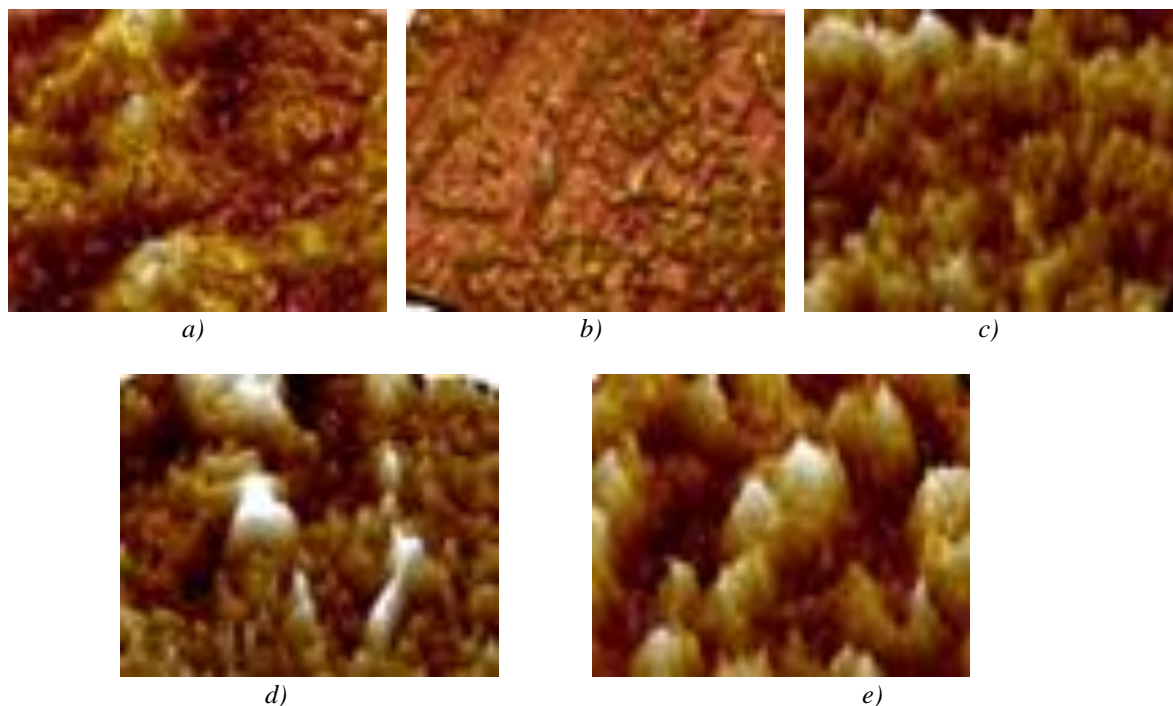


Fig. 12. Surface roughness of ZnO thin films irradiated at different doses.

(a) 0 kGy with RMS = 2.64 nm, (b) 5 kGy with RMS = 3.35 nm, (c) 15 kGy with RMS = 4.47 nm, (d) 20 kGy with RMS = 4.87 nm, (e) 25 kGy with RMS = 5.1 nm.

Fig. 12 represents the surface roughness of the ZnO films irradiated at various doses. As-deposited ZnO thin film has a roughness of 2.64 nm and gradually increased for the irradiated films (at 25kGy) up to 6.123 nm.

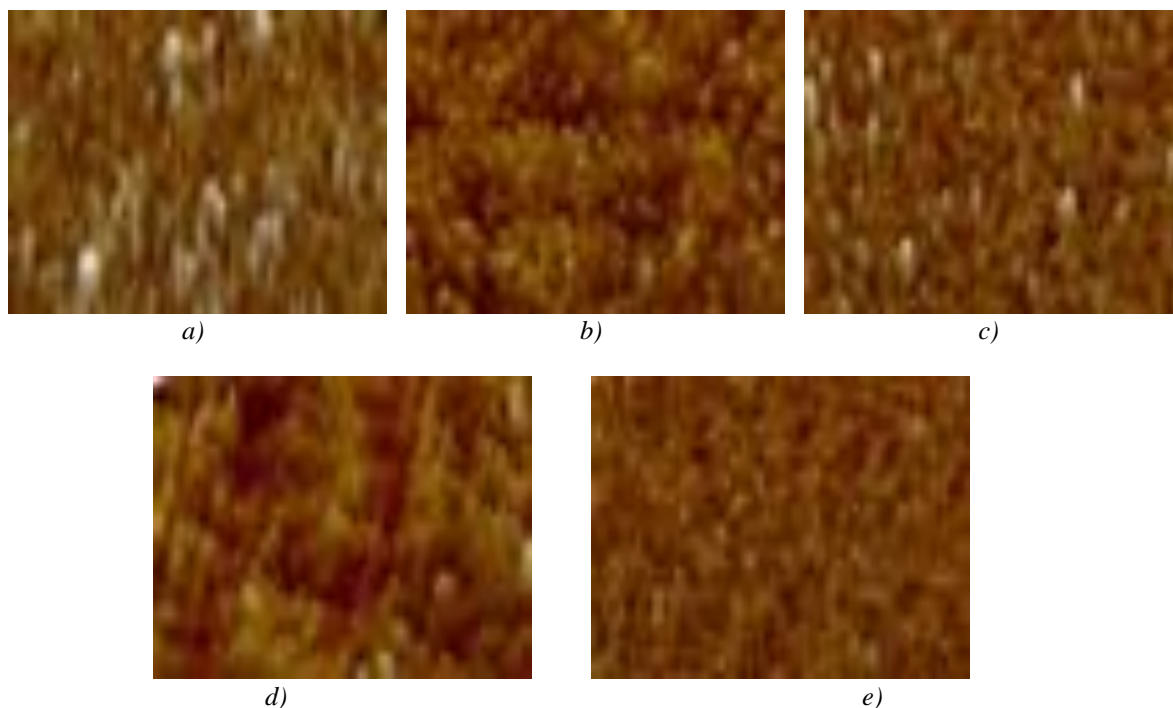


Fig. 13. The surface roughness of TiO₂ films irradiated at different doses.

(a) 0 kGy with RMS = 2.35 nm; (b) 5 kGy with RMS = 2.87 nm; (c) 15 kGy with RMS = 5.77 nm; (d) 20 kGy with RMS = 6.213 nm; (e) 25 kGy with RMS = 7.018 nm

The average surface roughness of the as-deposited TiO₂ films was observed to be in the range of 2.35 nm and gradually increased for the irradiated films (at 25 kGy) up to 7.018 nm as shown in fig. 13.

3.3. Optical energy gap

The band gap of TiO₂ and ZnO films were calculated from the optical spectra using the following equation (2):

$$Eg = h \frac{c}{\lambda} \quad (2)$$

The following is Table 2 which shows an example to calculate the optical band gap. Table 2. An example for the calculation of the band gap for the ZnO and TiO₂ thin films.

Band gap energy: $(Eg) = h \frac{c}{\lambda}$				
Planck's constant $h=6.626 \times 10^{-34}$ Joules sec				
Speed of light $c = 3.0 \times 10^8$ meter /sec				
Cut off wavelength $\lambda = 410.57 \times 10^{-9}$ meters. Example for (ZnO)				
<i>h</i>	<i>C</i>	λ	E	eV
6.63 E-34	3.0 E+8	4.11E-7	4.84 E-19	3.26
Where 1 eV=1.6×10 ⁻¹⁹ Joules.				

Table 2. shows the optical band gap values for the as-deposited and annealed TiO₂ and ZnO thin films. The decrease in the Energy gap due to the annealing can be explained by the improvement of the thin film structures and crystallinity for both materials. Furthermore, the decrease in energy band gap of the two oxides after the annealing of samples, can be attributed to an increase of the conductivity of the films.

Table 2. The energy band gap (E_g) values for as-deposited and annealed ZnO and TiO₂ thin films.

Energy gap (eV)	Sample
E = 3.26 eV	ZnO (as-deposited)
E = 3.01 eV	ZnO (annealed)
E = 3.76 eV	TiO ₂ (as-deposited)
E = 3.26 eV	TiO ₂ (annealed)

Table 3. Optical band gap (eV) versus radiation doses (kGy) for ZnO and TiO₂ films.

Dose	ZnO	TiO₂
0(kGy)	3.26	3.76
5(kGy)	3.02	3.7
10(kGy)	3.15	3.8
15(kGy)	2.93	3.56
20(kGy)	2.89	3.36
25(kGy)	2.89	3.8

The energy band gap decreases from ~ 3.26 eV for the freshly deposited ZnO film to ~ 2.89 eV for the film irradiated at 25 kGy dose. Many researchers have investigated the effects of gamma irradiation on numerous thin films. According to Abu EL-Fadl *and co-authors* who investigated the effect of gamma radiation on the band gap of $\text{Ag}_{10}\text{Te}_{90}$ thin films [14]. The authors attributed this to the radiation induced defect, increase of the absorption coefficient, followed by the absorption edge shifts to lower energies and narrow the optical band gap. This was supported by similar results found by Balboul *et al.* [15] and Chaudhury *et al* [16]. However, in a similar research field, Senthil and co-authors reported a decrease in the band gap of SnO thin films after gamma irradiation; they attributed this decrease to the increase in oxygen vacancies (V_O) which occurred just below the conduction band [17].

Fig. 14 shows the optical band gap of the ZnO and TiO₂ films versus irradiation doses up to 25 kGy.

In summary, for the TiO₂ films, the energy bad gap decreases from ~ 3.76 eV for the as-deposited film to ~ 3.36 eV for the film irradiated at 20 kGy dose. Then, it becomes 3.8 eV for the 25 kGy, further research is necessary to understand this sudden change in the band gap of the TiO₂ films. A summary of the optical band gap values is represented in table 3.

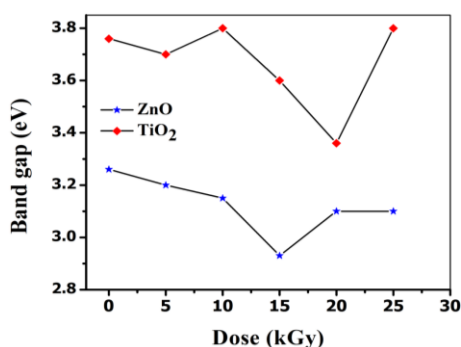


Fig. 14. Optical band gap (eV) versus radiation dose (kGy) for the zinc oxide and titanium dioxide films deposited on glass substrate

A summary of the transmission, optical band gap and roughness of the as-deposited ZnO and TiO₂ thin films is presented in Table 4.

Table 4. Typical properties and results obtained for the as-deposited TiO₂ and ZnO films.

(Results ZnO)	Results TiO ₂)	Property
85	75	Transmittance (%)
3.706	3.027	Optical Band gap (eV)
3.42	3.21	Surface Roughness (nm)
110	110	Thickness (nm)

3.4. Sheet resistance:

The resistivity ρ of the films was calculated from the simple equation $\rho = R_s d$, where d is the thickness of the film. By assuming that the thickness of the films is uniform, a low resistivity of ($2.25 \times 10^{-4} \Omega \cdot \text{cm}$) was measured for the 110 nm thick TiO₂ films at ambient temperature. While for 110 nm ZnO film the resistivity was ($2.10 \times 10^{-2} \Omega \cdot \text{cm}$).

The sheet resistance of the irradiated films remained the same for the various irradiation doses compared to the sheet resistance of the as-deposited films.

3.5. X-ray diffraction results of the ZnO and TiO₂ thin films

The effect of low gamma doses on the crystal structure of the samples was investigated

using the XRD method. Fig. 15 (a) represents the XRD patterns of the as-deposited ZnO films. It was noticed that there was no significant change in the intensity of the peaks for all examined ZnO samples (as-deposited and irradiated). The intensity of ZnO (101) diffraction peak at 22.5° , the second and the strongest was (004) peak at 33.6° , (200) at 42° , (440) at 52.1° and the fifth peak was at 60.5° for the (622) as seen in Fig. 15(a). Fig. 15(b) shows the XRD patterns of TiO₂ films irradiated at 10 kGy at room temperature. There was also no significant change in the patterns for the (as-deposited) 0kGy, 5kGy, 10kGy, 15kGy, 20 kGy and 25kGy of TiO₂ films. It shows the good quality of examined oxide films processed relatively low temperature growth (300°C). The intensity of TiO₂ (101) diffraction peak at 22° , was the strongest; the second intensity (004) peak was at 36.5° and the third one (200) was at 44° . As can be seen in figure 15(b), all diffraction peaks were very low, so higher deposition temperature may be necessary to improve the structural properties of TiO₂ films. Meanwhile, we could conclude that the ZnO and TiO₂ thin films obtained by PLD deposited at 300°C maintained polycrystalline structures even after low dose gamma irradiation.

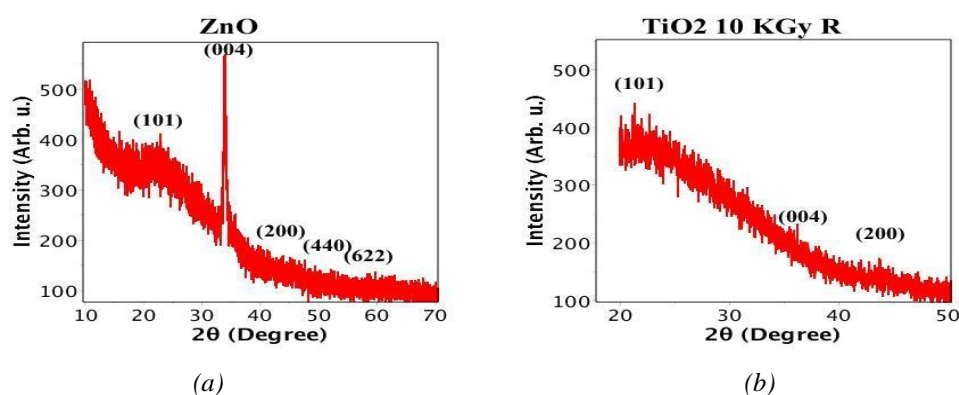


Fig. 15. XRD patterns of the: (a) ZnO and (b) TiO₂ films.

3.6. Energy dispersive X-ray spectroscopy (EDX)

To assess the elemental composition of the oxide films, EDX was performed on samples before and after irradiation. EDX analyses showed that Zn and O elements in the sample ZnO present in the solid film. The Si, Mg, and Ca elements that are not expected to be in solid films may probably result from the glass substrates. For the TiO₂ sample, elemental weight (wt.%) of Ti and O₂ are listed in Table 5.

Table 5. Elemental weight (wt.%) of Ti and O₂ are listed in Table 6.

	Zinc (wt.%)	Oxygen (wt.%)	Titanium (wt.%)
ZnO	51.0	48.80
TiO ₂	39.45	60.55

4. Conclusion

Average roughness R_a of the TiO₂ and ZnO deposited films was 3.2 nm and 3.42 nm respectively, for film thickness (110 nm). All deposited films were dense, and had good adhesion to glass substrates. AFM of both deposited films showed smooth surface and small grain sizes.

Optical spectral measured by a spectrophotometer showed high transmission of the deposited films (75-89%). Annealing the samples improved the surface roughness of the ZnO and TiO₂ films examined by the AFM. Effects of low dose ⁶⁰Co gamma irradiation on the morphological, structural, spectral and electrical characteristics of ZnO and TiO₂ were very small,

so the films maintained good structural and spectral properties; also morphology and low resistivity, even after low dose gamma irradiation.

For optoelectronic devices, high transparency, good conductivity and super smooth properties of TiO₂ and ZnO thin films are particularly desirable. Super-smooth and dense films are particularly desirable for solar cell device. The adhesion of deposited films onto substrates is directly dependent on the cleanliness of the substrate. All these properties could enhance their chemical stability of oxide films, especially when used in long term operation of a solar cell.

Acknowledgments

The authors would like to thank Imam Mohammad Ibn Saud Islamic University for the financial support of this project 351225.

References

- [1] Andreas Stadler, *Materials* **5**, 661 (2012).
- [2] M. Purica, E. Budianu, E. Rusu, M. Danila, R. Gavrilă, *Thin Solid Films* **403-404**, 485 (2002).
- [3] Y. W. Heo, D. P. Norton, S. J. Pearton, *J. Appl. Phys.* **98**(7), 073502 (2005).
- [4] M. G. Tsoutsouva, C. N. Panagopoulos, D. Papadimitriou, I. Fasaki, M. Kompitsas, *Materials Science and Engineering: B* **176**(6), 480 (2011).
- [5] N. Lehraki, M. S. Aida, S. Abed, N. Attaf, A. Attaf, M. Poulain, *Current Applied Physics* **12**(5), 1283 (2012).
- [6] Ping-Feng Yang, Hua-Chiang Wen, Sheng-Rui Jian, Yi-Shao Lai, Sean Wu, Rong-Sheng Chen, *Microelectronics Reliability* **48**(3), 389 (2008).
- [7] Jamilah Husnaa, M. Mannir Aliyua, M. Aminul Islama, P. Chelvanathana, N. Radhwa Hamzaha, M. Sharafat Hossaina, M. R. Karimc, Nowshad Amina, *Energy Procedia* **25**, 55 (2012).
- [8] W. L. Dang, Y. Q. Fu, J. K. Luo, A. J. Flewitt, W. I. Milne, *Superlattices and Microstructures* **42**, 89 (2007).
- [9] J. G. E. Gardeniers, Z. M. Rittersma, G. J. Burger, *J. Appl. Phys.* **83**, 7844 (1998).
- [10] H. Wang, T. Wang, P. Xu, *Journal of Materials Science: Materials in Electronics* **9**(5), 327 (1998).
- [11] M. G. Tsoutsouva, C. N. Panagopoulos, D. Papadimitriou, I. Fasaki, M. Kompitsas, *Materials Science and Engineering: B* **176**(6), 480 (2011).
- [12] E. Gyorgy, G. Socol, E. Axente, I. N. Mihailescu, C. Ducu, S. Ciuca, *Applied Surface Science* **247**, 429 (2005).
- [13] A. Al Yamani, N. Mustapha, *Thin Solid Films* **29**, 27 (2016).
- [14] A. Abu El-Fadl, M. M. Hafiz, M. M. Wakaad, A. S. Aashour, *Radiation Physics and Chemistry* **76**, 61 (2007).
- [15] M. R. Balboul, H. M. Hosni, S. A. Fayek, *Radiation Physics and Chemistry* **81**(12), 1848 (2012).
- [16] S. K. Chaudhuri, K. Goswami, S. S. Ghugre, D. Das, *J. Phys.: Condens. Matter* **19**(21), 216206 (2007).
- [17] V. S. Senthil Srinivasan, M. K. Patra, V. S. Choudhary, A. Pandya, *J. Optoelectron. Adv. M.* **9**(12), 3725 (2007).